The American Journal of Pathology, Vol. 175, No. 5, November 2009

DOI: 10.2353/ajpath.2009.090354

Stem Cells, Tissue Engineering and Hematopoietic Elements

Strain Differences in Behavioral and Cellular Responses to Perinatal Hypoxia and Relationships to Neural Stem Cell Survival and Self-Renewal

Modeling the Neurovascular Niche

Qi Li,* Jaimei Liu,* Michael Michaud,* Michael L. Schwartz,† and Joseph A. Madri*

From the Departments of Pathology and Neurobiology,† Yale University School of Medicine, New Haven, Connecticut*

Premature infants have chronic hypoxia, resulting in cognitive and motor neurodevelopmental handicaps caused by suboptimal neural stem cell (NSC) repair/recovery in neurogenic zones (including the subventricular and the subgranular zones). Understanding the variable central nervous system repair response is crucial to identifying "at risk" infants and to increasing survival and clinical improvement of affected infants. Using mouse strains found to span the range of responsiveness to chronic hypoxia, we correlated differential NSC survival and self-renewal with differences in behavior. We found that C57BL/6 (C57) pups displayed increased hyperactivity after hypoxic insult; CD-1 NSCs exhibited increased hypoxia-induced factor 1α (HIF-1α) mRNA and protein, increased HIF-1α, and decreased prolyl hydroxylase domain 2 in nuclear fractions, which denotes increased transcription/translation and decreased degradation of HIF-1α. C57 NSCs exhibited blunted stromal-derived factor 1-induced migratory responsiveness, decreased matrix metalloproteinase-9 activity, and increased neuronal differentiation. Adult C57 mice exposed to hypoxia from P3 to P11 exhibited learning impairment and increased anxiety. These findings support the concept that behavioral differences between C57 and CD-1 mice are a consequence of differential responsiveness to hypoxic insult, leading to differences in HIF-1α signaling and resulting in lower NSC proliferative/migratory and higher apoptosis rates in C57 mice. Information gained from these studies will aid in design and effective use of preventive therapies in the very low birth weight infant population. ***(Am J Pathol 2009, 175:2133–2145; DOI: 10.2353/ajpath.2009.090354)***

Preterm birth is known to result in cognitive and motor disabilities and recent evidence suggests that there can be significant recovery over time in some patients.[1–7] More than 1% of all live infants in the United States weigh less than 1000 g, and the survival rate for this population ranges from 60 to 85%.[8] The individuals that do survive exhibit a high rate of neonatal morbidities and are frequently severely compromised.[9,10] Many of these very low birth weight infants experience cerebral hypoxemia resulting from apnea and respiratory distress syndrome. Behavioral studies of this cohort have documented that approximately one quarter are functioning in the mentally retarded or borderline ranges at school age, 10% have cerebral palsy, and one half of these neonates need special assistance in school. The effects of hypoxia in the perinatal period include altered neuronal differentiation and synaptogenesis. The loss of neurons, glia, and their progenitor cells are thought to be the consequences of altered neuronal differentiation and synaptogenesis.[11] Interestingly, significant improvement in academic functioning over time in this population has been reported.[1] Although encouraging, this cognitive improvement is variable, and the repair/recovery mechanisms involved are not yet understood.

The variable recovery observed in the very low birth weight infant population may be a result of the responsiveness of neurogenic zones (neurovascular niches) in the brain, namely the subventricular zone and the subgranular zone, due to a range of responsiveness to the chronic hypoxic insult of hypoxia- induced factor 1α (HIF-1α) induction and its downstream signaling cascades. Consistent with this notion, investigators, using a murine

Supported in part by the U.S. Public Health Service (grants R37-HL28373 and R01-HL51018) and by a Reed Fellowship (to J.A.M.).

Accepted for publication July 16, 2009.

Address reprint requests to: Joseph A. Madri, Ph.D., M.D., Department of Pathology, Yale University School of Medicine, 310 Cedar St., P.O. Box 208023, New Haven, CT 06520-8023. E-mail: joseph.madri@yale.edu.

model mimicking the chronic hypoxia associated with premature birth, have demonstrated twice as many 5-bromo-2′-deoxyuridine-labeled cells expressing neuronal markers in the neocortex in mice recovering from hypoxia compared with normoxic-reared controls.[12] In addition, in both hypoxic-reared infant/juvenile mice, neuroblasts were noted detaching from the forebrain subventricular zone, migrating through the subcortical white matter, and entering the lower cortical layers several days after their last mitotic division.[12] These data suggest that neurogenesis probably plays a role in neuronal recovery after neonatal hypoxic injury. Observations made on adult mice demonstrating cortical, striatal, and hippocampal neurogenesis after a variety of injuries and responses to several treatment modalities are also consistent with this concept.[13] Thus, whereas neurogenesis after a hypoxic insult in the very low birth weight newborn may explain the cognitive improvement noted over time,[12] the variability of the improvement requires a better understanding of the mechanisms involved in modulating neurogenesis occurring in the subventricular zone (SVZ) before the development of treatment modalities geared to providing a greater and more complete recovery.

Our studies described here reveal that CD-1 NSC self-renewal ability is appreciably greater than that observed in C57BL/6 (C57) NSCs and that this may explain the differences in behavior observed in these two strains after exposure to hypoxia. Our previous findings documented significant differences in HIF-1α, brain-derived neurotrophic factor (BDNF), vascular endothelial growth factor (VEGF), stromal-derived factor 1 (SDF-1), neuropilin-1, and SDF-1 receptor CXCR4 protein expression in brain tissues and NSC lysates of these two strains. The current studies showed that CD-1 NSCs exhibit increased HIF-1α mRNA and protein levels and increased HIF-1α and decreased prolyl hydroxylase domain 2 (PHD2) proteins in their nuclear fractions compared with C57 NSCs. These data are consistent with increased levels of transcription and translation and decreased degradation of HIF-1α in the CD-1 NSCs. We also found that, compared with CD-1 NSCs, C57 NSCs exhibit blunted migratory responsiveness to SDF-1, decreased induction of matrix metalloproteinase (MMP)-9 and increased neuronal differentiation after migratory stimuli. Last, we demonstrated significant differences in SVZ vascular density, NSC proliferation, and selected behaviors in adult C57 mice compared with those in CD-1 adult mice after 8 days of hypoxic insult (10% O_2) at postnatal day (P) 3 to P11. This is consistent with our hypothesis that the behavioral data exhibited by the C57 pups is a consequence of their lower NSC proliferative and migratory rates and higher susceptibility to undergo apoptosis in response to a reduction in O_2% because of their relatively blunted HIF-1α response compared with that of CD-1 mice. The information gained from these and future studies will aid in the rational design and effective use of novel preventive therapies (directed at specific receptors and signaling pathway components) in the very low weight infant population.

Materials and Methods

Animal Model of Hypoxia

All animal studies were performed with approval and in full compliance with the Yale University Animal Care committee (protocol 2008-07366). CD-1 and C57BL/6 (C57) male and female breeders were obtained from Charles River Laboratories (Wilmington, MA) or laboratory stock derived from Charles River Laboratories breeders.[14] At P3 (approximates a 23-week gestational age in humans),[15,16] cohorts of mothers and pups were subjected to hypoxic (10% O_2) treatment; control mice remained under normoxic conditions as described.[12] Pups used for tissue analyses of SVZ NSC survival proliferation[14] were sacrificed at P11 (approximates a full-term gestation in humans).[15,16] Mice to be used for behavioral analysis were exposed in the same manner between P3 and P11 and were then kept under normoxic conditions from P12 until the completion of testing.

Behavioral Testing

All behavioral testing was performed exclusively on males. We recognize that gender effects on behavior in rodents have been documented[17] and is a potential limitation of our interpretations of this study.

Reflex Activity

The righting and whisker-orienting reflexes and forelimb placing were assessed on P12. The righting reflex was tested by placing the animal on its back and assessing the time and ability to turn over and right to all four feet. The whisker-orienting reflex was assessed by brushing the whiskers with a small brush. Normal mice stop moving the whiskers when touched and will orient the head to the side touched. Finally, forelimb placing was examined by holding the animal by the body and bringing the hanging forelimbs in contact with the tabletop and observing the extension of the forelimbs to the surface of the tabletop.

Open-Field Activity

Spontaneous open-field behavior was evaluated in mice between P18 and P19. Nineteen normoxic (9 CD-1 and 10 C57) and 23 hypoxic (11 CD-1 and 12 C57) mice were tested by placing them in a Plexiglas enclosed open field (25 $\times$ 25 $\times$ 40 cm) equipped with infrared photo beams coupled to a computer running TruScan software (Coulbourn Instruments, Whitehall, PA) to automatically record movements within the field. Activity was monitored during a single 28-minute session and measures of total distance moved (cm/4 minutes), the average velocity of movements (cm/1 minute), the amount of time without movement (rest time; seconds/4 minutes), and center time were recorded. Data were binned into three 4-minute intervals and were analyzed using a multiple analysis of variance test with repeated measures.

Free-Swim Test

At 4 months of age mice were assessed using the free-swim task. This test assesses behavioral laterality and cerebral asymmetries and is particularly sensitive to the organization and integrity of the corpus callosum linking the two hemispheres.[18–20] Mice were tested for 5 minutes in each of three test sessions spaced approximately 48 hours apart. In each session the mouse was placed in the center of a tank of water with a depth of 33 cm and measuring 33 cm in diameter. The swimming activity of the mouse was videotaped and the amount of movement in the clockwise and counterclockwise directions, changes in the direction of swimming and the consistency of preferred swimming direction across sessions was analyzed in 30-degree increments. Each swimming activity of 30 degrees was scored as a turn in a given direction (clockwise or counterclockwise).

Morris Water Maze

Mice were assessed using the water maze between 3 and 5 months of age. This test provides an assessment of learning and memory abilities related to hippocampal and cortical memory systems.[21] Mice were given four trials per day for 8 consecutive days to find and swim to a transparent Plexiglas platform hidden just below the surface of the water within one quadrant of a circular opaque plastic tub (1.5 m in diameter). A video tracking system (Coulbourn Instruments) monitored the path and time to reach the platform for each trial. To assess the strength of initial learning, a 60-second probe trial was given on the 9th day during which the hidden platform was removed. The total path length, % time spent in the platform (training) quadrant, and the probe preference score (PPS) were calculated from the video records. Probe preference reflects the time spent in the training quadrant (T) relative to time in the other three quadrants (opposite, right, and left) on the probe trial. The PPS is equal to $[(T - O) + (T - R) + (T - L)]/3$.

NSC Isolation and Culture

NSCs were isolated from the brains of P1 C57 and CD-1 pups as described and cultured in NSC medium (Dulbecco's modified Eagle's medium/F12 supplemented with N-2 [Gibco, Carlsbad, CA], 20 ng/ml of epidermal growth factor, 10 ng/ml basic fibroblast growth factor, 1% L-glutamine, 1% penicillin/streptomycin, and Fungizone) and incubated in 5% CO_2 at 37°C.[14] Primary cultures were incubated for 15 to 20 days, at which time neurospheres form. The NSCs were plated at 1×10^4 or 1×10^5 cells/ml and plated into six-well cluster plates and cultured under either normoxic or hypoxic (5%O_2) conditions for 6 days.

Although our *in vivo* model of murine chronic sublethal hypoxia mimics the human counterpart, moving to *in vitro* models, although valuable and useful for elucidating mechanisms, should be approached with the knowledge that any *in vitro* culture conditions will elicit changes in cell-cell and cell-matrix interactions and changes in metabolism that can influence any data accrued. Further, standard tissue culture conditions are usually set at 20% O_2, a hyperoxic environment. Our approach to this concern has been to assess whether the endothelial cells and NSCs that we use are capable of resetting their normoxic set point when grown in a range of O_2 percentages and exhibit induction of HIF-1α in response to lowering O_2% values over a range of O_2 percentages as has been recently demonstrated.[22] Indeed, we have observed that our NSCs are capable of this and exhibit induction of HIF-1α when O_2% is changed from 20 to 10%, from 10 to 5%, and from 20 to 5% as illustrated in Figure 1, A–G. When O_2% was changed from 5 to 1% considerable apoptosis was observed (not shown).

In light of these studies illustrating similar HIF-1α inductions (and BDNF [not shown]) as well as graded effects on proliferation and apoptosis when O_2% was changed from 20 to 10%, 20 to 5%, and from 10 to 5% and good correlation between our previously published *in vivo* and *in vitro* studies,[14] we elected to use a 20 to 5% reduction in O_2% for our *in vitro* studies. In addition, when C57 and CD-1 NSC apoptosis (assessed using cleaved caspase 3) and proliferation (assessed using proliferating cell nuclear antigen [PCNA]) were investigated at various O_2 levels we observed that C57 NSCs appeared to be more sensitive to reductions in O_2% compared with CD-1 NSCs, exhibiting increased cleaved caspase 3 and decreased PCNA expression levels as O_2% was reduced from 20 to 10% and from 10 to 5%.

Endothelial Cell Culture

Immortalized mouse C57 wild-type brain endothelial cells (BECs) were obtained from Dr. Britta Engelhardt (The Theodor Kocher Institute, Bern, Switzerland) and cultured with BEC medium (Dulbecco's modified Eagle's medium and 10% fetal bovine serum, 1% L-glutamine,1% nonessential amino acid, 1% sodium pyruvate, 1% HEPES, and 10^{-5} M β-mercaptoethanol) and incubated in 8% CO_2 at 37°C as described previously.[23–25]

RT-PCR

Total RNA of CD-1 and C57 NSCs was isolated with TRIzol (Invitrogen, Carlsbad, CA). A real-time quantitative RT-PCR was performed using the iCycler iQ system (Bio-Rad Laboratories, Hercules, CA). cDNA was prepared, starting from 1 μg of total RNA using the iScrypt cDNA Synthesis Kit according to the manufacturer's instructions. PCR reactions for HIF-1α were performed with the following primer set: sense primer 5′-TGTGAACCCATTCCTCATCCGTCA-3′ and antisense primer 5′-TCCGGCTCATAACCCATCAACTCA-3′. Primers for the internal control, glyceraldehyde-3-phosphate dehydrogenase were included in each reaction: sense primer 5′-TCCAGTATGATTCCACCCATGGCA-3′ and antisense primer 5′-ACGTACTCAGTGTCAGCATCACCA-3′. PCR was performed using iQ SYBR Green Supermix (Bio-Rad Laboratories) in a final volume of 25 μl, starting with a

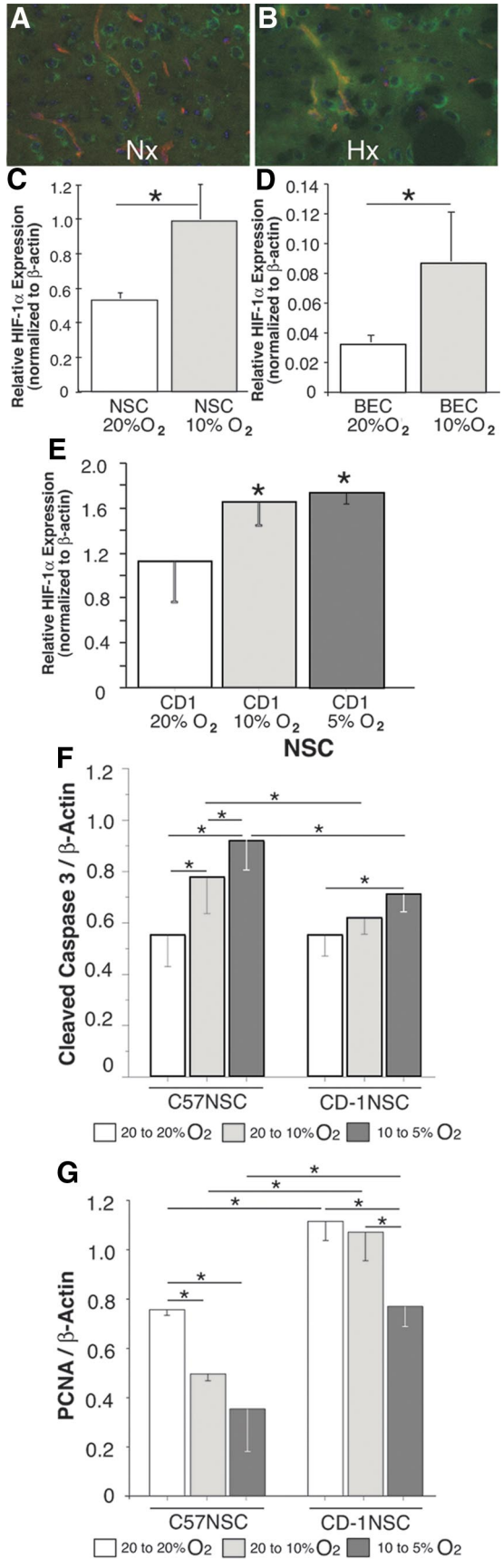

3-minute template denaturation step at 95°C followed by 40 cycles of 95°C for 30 seconds and 55°C for 30 seconds.

Immunoblotting

NSCs were homogenized in lysis buffer composed of 50 mmol/L Tris-HCl, pH 7.4, 150 mmol/L NaCl, 1% Nonidet P-40, 10% glycerol, 1 mmol/L sodium orthovanadate, 1 mmol/L phenylmethylsulfonyl fluoride, and protease inhibitor cocktail (Boehringer Mannheim GmbH, Mannheim, Germany). Equal amounts of total protein (20 μg) were run on 10 or 12% SDS-polyacrylamide gels, transferred to polyvinylidene difluoride membranes, and immunoblotted with antibodies according to the manufacturer's instructions. Antibodies used included rabbit anti-HIF-1α (1:200), anti-PHD2 (Novus Biologicals, Inc., Littleton, CO), anti-phospho mammalian target of rapamycin (mTOR), anti-mTOR, anti-phospho AKT, anti-AKT, anti-phospho P70, anti-P70, anti-phospho eIF4E, anti-eIF4E, anti-phospho p4E-BP1, and anti-p4E-BP1 at a dilution of 1:1000 (Cell Signaling Technology, Danvers, MA); anti-cleaved caspase 3; anti-PCNA; (Cell Signaling Technology, Danvers, MA) and anti-β-actin (1:1000; Santa Cruz Biotechnology, Inc., Santa Cruz, CA). Bound antibodies were detected by using horseradish peroxidase-conjugated anti-IgG (Cell Signaling Technology) and a chemiluminescence detection system as described previously.[25] Quantitation was performed on scanned densitometric images (Agfa Arcus II Scanner with Adobe Photoshop CS, Adobe Systems, Beaverton, OR) using Quantity One software (Bio-Rad Laboratories). Western blot data are expressed as histograms of averages of relative levels (in arbitrary units) of at least three independent determinations for each protein examined.

Immunohistochemistry

Neurospheres were fixed with 4% paraformaldehyde in PBS, pH 7.2, for 10 minutes. Immunofluorescence staining was performed with the following antibod-

Figure 1. A and **B:** SVZ BEC and NSC HIF-1α induction by hypoxia *in vivo*. Double labeling with anti-CD31 (red fluorescence) and anti-HIF-1α (green fluorescence) reveals a low baseline HIF-1α expression in SVZ vasculature and neuropils under normoxia (Nx) (slight orange fluorescence in the vascular compartment and a slight green fluorescence in the neuropil), which is induced after hypoxia (Hx) (intense orange fluorescence in the vascular compartment and increased green fluorescence in the neuropil). **C** and **D:** CD-1 NSCs (**C**) and BECs (**D**) cultured in 20% O_2 and moved to 10% O_2 exhibited similar inductions of HIF-1α. $n = 3$; $^*P < 0.05$. **E:** NSCs cultured at 20% O_2 (white bar, CD-1 20% O_2), NSCs cultured at 20% O_2 and moved to 10% O_2 (light gray bar, CD-1 10% O_2), and NSCs cultured at 10% O_2 and moved to 5% O_2 (dark gray bar, CD-1 5% O_2) exhibited similar inductions of HIF-1α, whereas NSCs cultured at 5% O_2 and moved to 1% O_2 exhibited considerable apoptosis and no induction of HIF-1α (not shown). $n = 3$; $^*P < 0.05$. **F:** C57 and CD-1 NSCs cultured at 20% O_2 and kept at 20% exhibit similar cleaved caspase 3 levels. On reduction of O_2% from 20 to 10%, the C57 NSCs exhibited increased cleaved caspase 3 expression, whereas the CD-1 NSCs did not. On reduction of O_2% from 10 to 5%, both the C57 and the CD-1 NSCs exhibited increased expression of cleaved caspase 3, with the C57 NSCs exhibiting the higher levels. $n = 6$; $^*P < 0.05$. **G:** CD-1 NSCs cultured at 20% O_2 and kept at 20% expressed higher PCNA compared with C57 NSCs, as expected. On reduction of O_2% from 20 to 10% the C57 NSCs exhibited decreased PCNA expression, whereas the CD-1 NSCs did not. On reduction of O_2% from 10 to 5% both the C57 and the CD-1 NSCs exhibited decreased expression of PCNA, with the C57 NSCs exhibiting the greater reduction. $n = 6$; $^*P < 0.05$.

ies against mouse nestin (1:200, BD Pharmingen, San Diego, CA), glial fibrillary acidic protein (GFAP) (1:200, Sigma-Aldrich, St. Louis, MO), and β-tubulin III (1:200, Sigma-Aldrich). Secondary antibodies were goat anti-rabbit 594 and goat anti-mouse Alexa Fluor 488 (1:200, Molecular Probes, Eugene, OR). Coverslips were mounted with Vectashield (with 4,6-diamidino-2-phenylindole), and specimens were imaged using confocal microscopy. Confocal images were obtained using a laser-scanning confocal microscope (FluoView, Olympus, Tokyo, Japan) integrated with a microscope (IX70-S1F2, Olympus) with LCPlanFl ×40 NA 0.60 objectives (Olympus) and were acquired using FluoView software (Olympus).

NSC Migration Measurement

We used the three rapid procedures described by Durbec et al[26] to test the effect of specific factors on the NSC migration process.

Chemotaxis Assay

Chemotaxis assays were performed with BD Biocoat growth factor reduced Matrigel invasion chambers (8-μm-pore Transwells, BD Sciences, San Jose, CA). C57 and CD-1 neurospheres were dissociated with 0.1% trypsin and then 2.5×10^4 cells were placed in the wells of the upper compartments of 8-μm-pore Transwell chambers, with the lower compartment containing NSC medium without or with SDF-1 for 24 hours.

For the coculture assays, 1×10^5 BECs in 500 μl of BEC medium were added to the lower chambers for 4 hours. The wells were washed with PBS twice and then 2.5×10^4 CD-1 or C57 NSCs were added to the upper chamber with 500 μl of NSC medium including 1 μg/ml anti SDF-1. After 24 hours, the cells on the upper side of the membrane were removed with a cotton swab. The cells on the lower surface of the membrane were air-dried, fixed, and stained with 4,6-diamidino-2-phenylindole. Six random selected ×10 magnification microscopic fields of each membrane were counted and three inserts were counted per condition with the average value was taken as the final result.

Radial Migration Assays

CD31 brain-derived microvascular endothelial cells (2×10^4) were seeded in 24-well plates and cultured with BEC medium overnight. On the second day the BEC medium was removed, and the BECs were washed once with 1× PBS buffer. Individual C57 and CD-1 neurospheres of approximately the same size (80 to 100 μm in diameter) were selected, gently plated in the center of each well, and covered with 500 μl of NSC medium with or without exogenous SDF-1 (10 ng/ml) or anti SDF-1 (1 μg/ml). The plates were incubated at 37°C in a 5% CO_2-humidified incubator. Images were captured at 48 hours with an Olympus IX71 fluorescence microscope using an Optronics Microfire C camera. Distances covered by cells migrating out of the neurosphere were measured by using NIH ImageJ. Three independent experiments were performed, for which each data point is a pool of 12 to 14 neurospheres.

Chain Migration Assays

Brains from 10-day-old CD-1 and C57 mouse pups were harvested and Vibratome-sectioned. Frontal sections containing the SVZ were placed in Petri dishes; SVZ fragments were then dissected out, cut into small pieces (~0.2 mm), and embedded in Matrigel in four-well cluster dishes. Four explants/dish were arranged in the Matrigel, and 500 μl of medium was added to cover the three-dimensional gel. To test the effect of SDF-1 on the migration of NSCs in both CD-1 and C57 isolated SVZs, exogenous SDF-1 (10 ng/ml) or anti SDF-1 (1 μg/ml) was added to the culture medium separately. Forty-eight hours after culture, the neuronal precursors were observed to migrate radially out of the explants in chain-like organizations, forming a complex three-dimensional network. Migration quantification was obtained by a direct measurement of cell migration around the explants from the border of the explant to the migration front under microscopy using an Olympus IX71 fluorescence microscope with an Optronics Microfire C camera. Distances covered by chains of cells migrating out of the nSVZs were measured by using NIH ImageJ. Eight measurements were performed on each sample and *n* SVZ explants per condition were analyzed. The averages of the distances were calculated.

SDS-PAGE Zymography

Conditioned media were collected and concentrated using Centricon concentrators (30,000 molecular weight cutoff) (Millipore, Bedford, MA), protein concentrations were determined with a Bio-Rad system. Equal amounts of protein (20 μg) for each sample were mixed with 3× sample buffer and loaded on a 10% polyacrylamide gel incorporated with 0.1% gelatin for electrophoresis. After electrophoresis, gels were washed in 2.5% Triton X-100 for 1 hour, incubated overnight at 37°C in collagenase buffer, and stained for 1 hour with 0.1% Coomassie Brilliant Blue. Gelatinolytic activity was visualized as a transparent band against a blue background. Quantitation was performed using Quantity One software. Duplicate samples incubated with EDTA served as collagenase controls.[27–29]

Statistical Analysis

All experiments were repeated at least three times. The statistical significance of differences was evaluated by Statview 5.0 using N-way analysis of variance (SAS Institute, Cary, NC), and significance was taken as $P < 0.05$. Statistical significance is denoted by the horizontal lines (SDs) and associated *P* values above pairs of individual columns in the figures.

Table 1. C56BL/6 and CD-1 NSC Normoxic and Hypoxic Proliferation and Apoptosis

	P11 NSC proliferation (%)		P11 NSC apoptosis (%)	
	Normoxia	Hypoxia	Normoxia	Hypoxia
C57	20.6 ± 8.0	8.6 ± 1.5	6.7 ± 2.5	30.0 ± 6.0
CD-1	30.2 ± 7.2	21.2 ± 2.7	2.8±1.0	14.7 ± 7.2

Our previous studies[14] revealed a higher proliferation of CD-1 NSCs compared with those of C57BL/6 pups (30.2% versus 20.6% [$P < 0.05$] in normoxia and 21.2% versus 8.6% [$P < 0.05$] in hypoxia [10% O_2]), indicating that CD-1 NSC self-renewal ability is greater than that observed in C57BL/6 NSCs. In addition, cleaved caspase 3 staining and Western blots showed that C56BL/6 NSCs exhibited significantly increased apoptosis in SVZ tissue (6.7% versus 2.8% [$P < 0.05$] in normoxia [20% O_2] and 30.0% versus 14.7% [$P < 0.05$] in hypoxia [10% O_2]) and in culture under hypoxic conditions (not shown) than CD-1 NSCs. $n = 6$. Data from Ref.[14]

Results

Our previous data showed that CD-1 P3 pups survive a 30-day exposure to hypoxia (9.5% O_2), whereas C57BL/6 pups expire at day 13 under similar conditions. CD-1 and C57BL/6 pups reared under hypoxic conditions have significantly lower body weights ($P < 0.05$) at the midpoint and end of the hypoxic period than normal controls. By P11, the mean weight of CD-1 hypoxic mice is 72% of that of CD-1 controls and weight of hypoxic C57BL/6 mice is 60% of that of controls. In this model the hypoxia-induced changes in brain weight are indistinguishable from those of normoxic mice.[12] *In vivo* data revealed a higher baseline proliferation of CD-1 NSCs compared with those of C57BL/6 pups, indicating that CD-1 NSC self-renewal ability is greater than that observed in C57BL/6 NSCs. In addition, cleaved caspase-3 staining and Western blots showed that C57BL/6 NSCs exhibited significantly increased apoptosis in SVZ tissue and in culture under hypoxic conditions compared with that in the CD-1 mice NSCs (Table 1).[14]

Neither C57 or CD-1 mice exposed to hypoxia between P3 and P11 exhibited significant differences in the presence or execution of the righting, forelimb placing, and whisker orientation reflexes compared with age-matched normoxic mice. Assessment of open-field behavior revealed that C57 mice reared under hypoxia exhibited significantly increased locomotor activity (hyperactivity) on measures of the total distance traveled, the velocity of movements, center time, and rest time compared with normoxic controls (Table 2).

In contrast, CD-1 mice showed no significant differences between hypoxic and normoxic conditions on any measure of activity at P16 to P18 (CD-1 normoxic and hypoxic data, Table 2). These data suggest a correlation of behavioral recovery with SVZ NSC self-renewal and survival capabilities of these two mouse strains.

CD-1 and C57 NSCs Exhibit Different Levels of HIF-1α Translation, Expression, and Activation in Normoxia and After Hypoxic Insult

Particular strains of mice can exhibit a variety of responses to specific insults. This has been observed in comparisons of the CD-1 and C57 strains after hypoxic insults. Specifically, after middle cerebral artery occlusion, the CD-1 mice do not recover as well as the C57 mice.[30] However, after a sublethal chronic hypoxic insult we and others have found that the CD-1 mice exhibit a more robust recovery compared with C57 mice (examining physiological parameters, HIF-1α, and downstream signaling pathway components, angiogenesis, NSC proliferation, and apoptosis).[14,31]

These data prompted us to investigate whether these biochemical and behavioral differences would be correlated with HIF-1α mRNA and/or protein levels and subcellular localization. Real-time RT-PCR and Western blot data revealed that HIF-1α mRNA was higher in CD-1 NSC lysates than in C57 NSC lysates after reduced O_2 conditions (Figure 2A), whereas HIF-1α protein expression was higher in CD-1 NSC lysates compared with C57 NSC lysates under both 20% and 5% O_2 culture conditions (Figure 2B).

In addition to the increases in HIF-1α mRNA and protein levels in CD-1 NSCs, the subcellular localization profiles (cytoplasmic versus nuclear) of HIF-1α and PHD2 were significantly different in NSCs of the two strains (Figure 2, C and D). Namely, the nuclear (active) fraction of HIF-1α was increased in CD-1 NSCs cultured in both 20% and 5% O_2 conditions, whereas the nuclear fraction of PHD2 was found to be significantly higher in C57 NSCs cultured in both culture conditions, suggesting

Table 2. C56BL/6 and CD-1 NCS Open-Field Activity

	P16–18 activity measures in a 28-minute session (SD)			
Strain and group	Total distance (cm/4 minutes)	Velocity (cm/min)	Rest time (seconds/4 minutes)	Center time (seconds/4 minutes)
CD-1 normoxic ($n = 9$)	710 (103)	177 (26)	98 (10)	49 (13)
CD-1 hypoxic ($n = 11$)	645 (104)	161 (26)	106 (12)	43 (21)
C57BL/6 normoxic ($n = 10$)	408 (61)	102 (15)	128 (12)	109 (60)
C57BL/6 hypoxic ($n = 12$)	485 (98)*	121 (24)*	124 (14)	60 (35)*

After hypoxic exposure from P3 to P11 spontaneous open-field behavior was examined between P16 and P18 over a 28-minute session. Comparison of C57BL/6 normoxic and hypoxic mice revealed a significant increase in activity for hypoxic mice. Measure of total distance moved, and the average velocities of movements were significantly increased ($P < 0.05$), whereas the time spent in the center of the arena (approximately the central two thirds) was significantly decreased. The latter observation is consistent with a greater level of anxiety or fearfulness. Comparison of CD-1 normoxic and hypoxic mice revealed no significant differences in any measure of activity. These data are consistent with the differential SVZ NSC self-renewal and survival.

*$P < 0.05$.

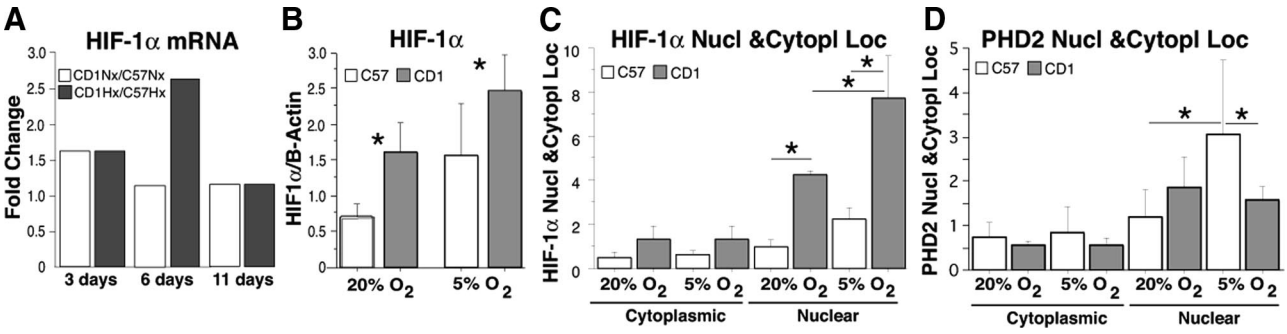

Figure 2. A and **B:** Reduced O_2 culture conditions increased HIF-1α mRNA and protein expression in CD-1 NSCs, but not in C57 cells. **A:** C57 and CD-1 NSCs were incubated in reduced O_2 culture conditions (5% O_2) for 3, 6, and 11 days, and the mRNA levels of HIF-1α were analyzed by RT-PCR. **B:** The protein levels of HIF-1α in NSCs were analyzed by Western blot after 6 days of reduced O_2 culture conditions (5% O_2). $n = 3$; $^*P < 0.05$. **C** and **D:** The cytoplasmic and nuclear fractions of C57 and CD-1 NSCs were isolated after 6 days of reduced O_2 culture (5% O_2). The protein levels of HIF-1α (**C**) and PHD2 (**D**) in cytoplasmic and nuclear fractions were detected by Western blot. $n = 3$; $^*P < 0.05$.

increased HIF-1α protein expression and decreased HIF-1α hydroxylation in the CD-1 NSCs.

To further elucidate the mechanisms involved in modulating HIF-1α expression levels in these two murine strains after hypoxic insult we examined the elements involved in control of protein translation. Specifically, we found that after a hypoxic insult (20% O_2 to 5% O_2) CD-1 Akt, mTOR, P70, eIF4E, and 4E-BP1 exhibited increased levels of phosphorylation, consistent with increased protein (HIF-1α) translation (Figure 3, A–H). Interestingly, inhibition of mTOR with rapamycin in both C57 and CD-1 NSC cultures grown at 20% O_2 and reduced O_2 (5% O_2) inhibited mTOR and 4E-BP1 phosphorylation and HIF-1α expression, suggesting that NSC translational responsiveness to a reduced O_2 environment is, in part, mTOR-dependent (Figure 3, F–H). These data suggest that CD-1 NSCs exhibit increased HIF-1α protein expression and decreased HIF-1α hydroxylation (inactivation) compared with C57 NSCs after hypoxic insult, possibly resulting in decreased levels of CD-1 NSC apoptosis and increased levels of CD-1 NSC proliferation.

C57 and CD-1 NSCs Exhibit Differential Signaling and Migration Responses to SDF-1

In our previous studies we documented differences in CXCR4 expression in C57 and CD-1 brain homogenates and cultured C57 and CD-1 NSCs, with CD-1 brain homogenates exhibiting a 1.6-fold increase in CXCR4 ex-

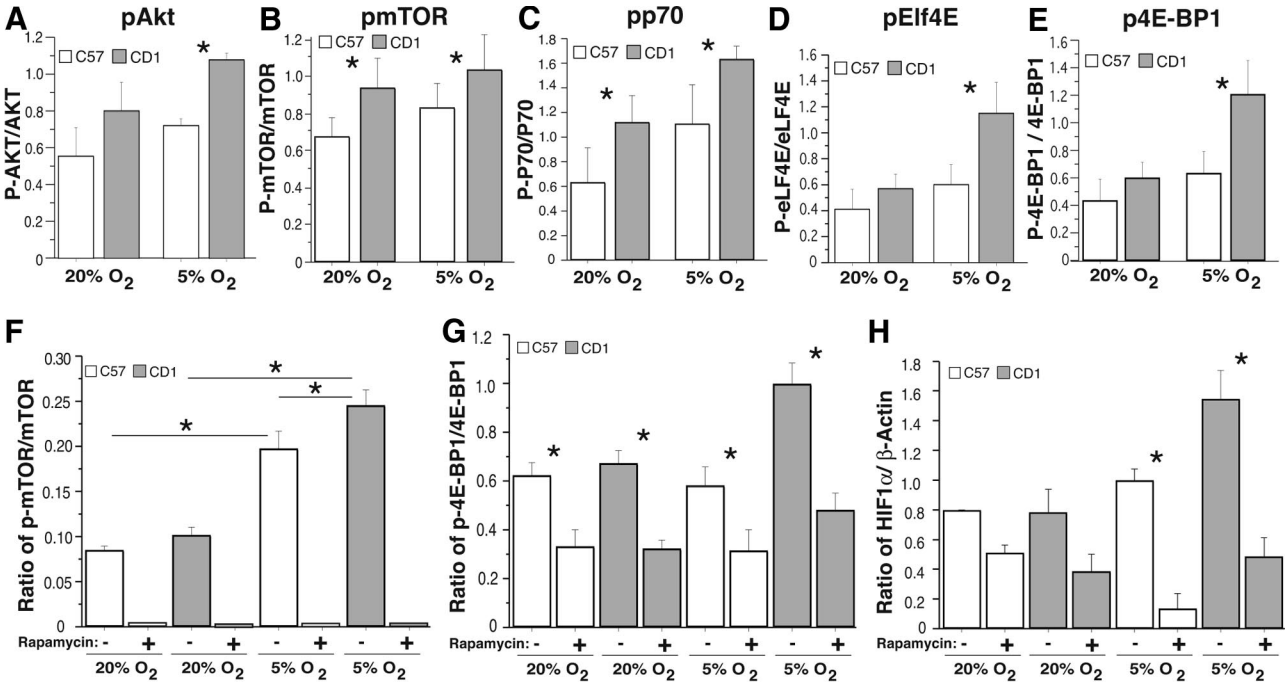

Figure 3. A–E: Elements modulating protein translation levels in C57 (open boxes) and CD-1 (shaded boxes) mice. Western blots of C57 and CD-1 NSC AKT (**A**), mTOR (**B**), p70 (**C**), eIf4E (**D**), and 4E-BP1 (**E**) all exhibited increased phosphorylation after 6 days of reduced O_2 (5% O_2). $n = 3$; $^*P < 0.05$. **F–H:** Western blots of C57 (open boxes) and CD-1 (shaded boxes) NSC pmTOR/mTOR (**F**), p4E-BP1/4E-BP1 (**G**), and HIF-1α/β-actin (**H**) in the absence (−) and presence (+) of rapamycin, illustrating inhibition of mTOR phosphorylation and a blunting of 4E-BP1 phosphorylation and HIF-1α expression in the presence of rapamycin after 6 days of normoxia (20% O_2) and reduced O_2 (5% O_2). $n = 3$; $^*P < 0.05$.

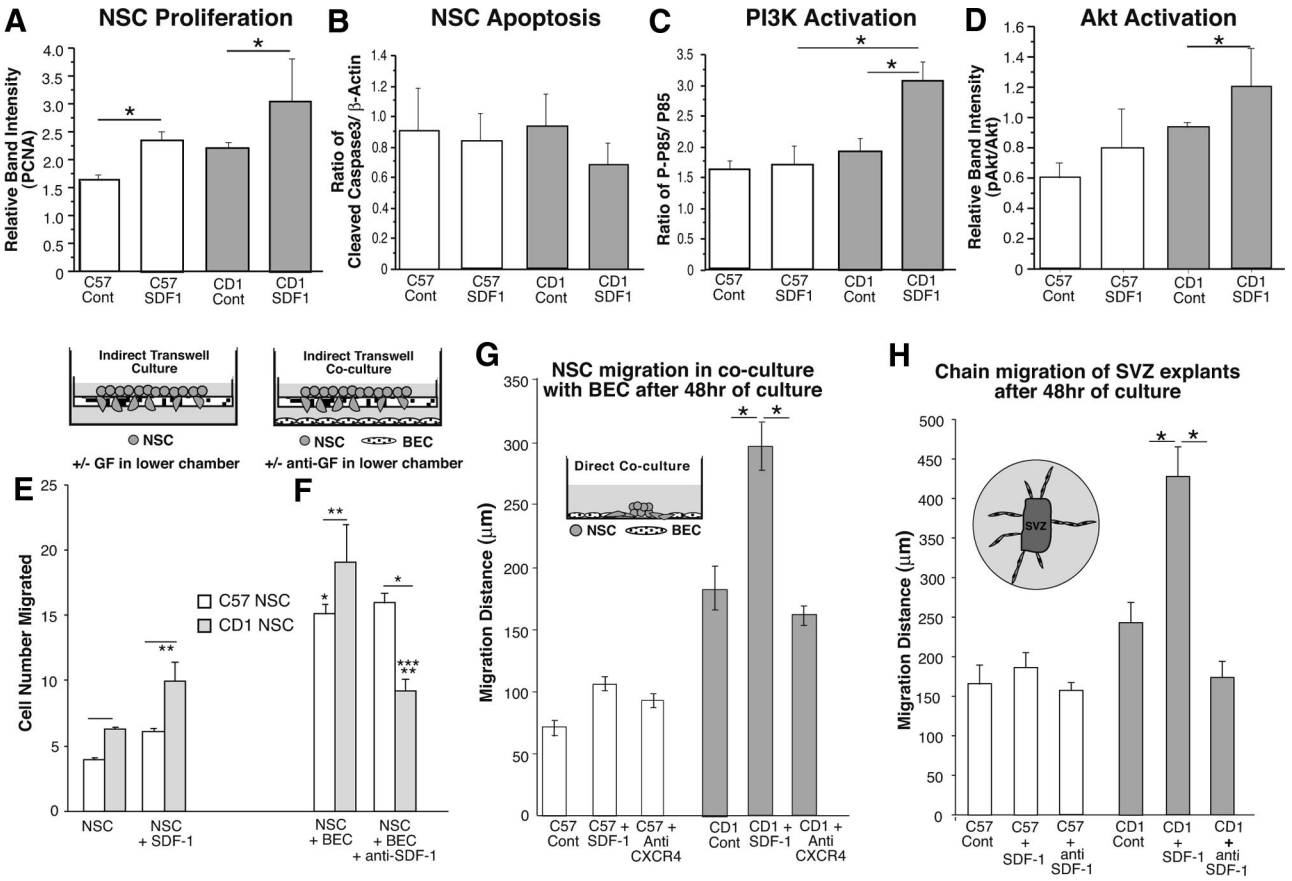

Figure 4. A and **B:** Western blots of C57 and CD-1 NSC lysates illustrating averaged PCNA (**A**) and cleaved caspase 3 (**B**) expression under baseline conditions and in response to rSDF-1 (normalized to β-actin). $n = 3$; $^*P < 0.05$. **C** and **D:** Western blot comparisons of C57 and CD-1 NSC lysate pp85/p85 PI3K (**C**) and pAKT/Akt (**D**) relative ratios illustrating baseline levels and after induction by rSDF-1. $n = 3$; $^*P < 0.05$. **E–H:** SDF-1 responsiveness plays an important role in the differential regulation of CD-1 and C57 NSC migration. **E:** Chemotaxis assay. Dissociated neural cells placed in the wells of the upper compartments of 8-μm-pore Transwell chambers, with the lower compartment containing medium without or with SDF-1 for 24 hours. $^*P < 0.05$ vs. C57 NSC; $^{**}P < 0.05$ vs CD1 NSC; $^{***}P < 0.05$ vs. CD1 NSC + BEC. **F:** Dissociated neural cells placed in the wells of the upper compartments of 8-μm-pore Transwell chambers, with the lower compartment containing brain-derived microvascular endothelial cells in medium without or with anti-SDF-1 for 24 hours. Cells situated on the lower side of the filter are fixed, stained, and counted. **G:** Radial migration analysis of individual neural spheres cocultured with subconfluent brain-derived microvascular endothelial cells in medium without or with either SDF-1 or anti-SDF-1 for 48 hours. **H:** Chain migration assay. Single SVZ tissues harvested from P15 pups were embedded in Matrigel and cultured in medium without or with either SDF-1 or anti-SDF-1. After 3 days, radial chain migration of neurites was measured. $n = 3$; $^*P < 0.05$. Cont, control. GF, growth factor.

pression compared with C57 brain homogenates under reduced O_2 conditions (10% O_2). In addition, CD-1 NSCs expressed a 1.3-fold increase in CXCR4 protein compared with C57 NSCs under 20% O_2 culture conditions and a 1.6-fold increase in CXCR4 protein compared with C57 NSCs under 10% O_2 culture conditions.[14] To assess what effect this may have on C57 and CD-1 NSC survival, proliferation, and migration, we treated the NSCs with recombinant (r) SDF-1 or anti-SDF-1 and measured the effects on survival, proliferation, and migration in mono- and coculture with BECs as illustrated in Figure 4, A–H.

Figure 4A demonstrates significant increases in PCNA expression after SDF-1 treatment observed in C57 and CD-1 NSCs ($P < 0.05$).[14] In contrast, no differences in cleaved caspase 3 were observed at baseline conditions or after rSDF-1 treatment (Figure 4B).

To better understand the underlying signaling mechanisms engaged by activation of the CXCR4 receptors in the NSCs isolated from these two mouse strains, we assessed the phosphorylation states of the signaling components known to be activated after SDF-1 engagement of CXCR4, specifically phospho (p)-phosphatidylinositol 3-kinase (PI3K), pAkt, phospho-extracellular signal-regulated kinase, and pp38, whose activations are thought to modulate survival, proliferation, adhesion, migration, and differentiation after CXCR4 engagement.[32–36]

As seen in Figure 4, C and D, although there were no significant differences in p85 activation and a nonstatistically significant trend in Akt activation after SDF-1 treatment observed in C57 NSCs, there was a significant increase in CD-1 NSC p85 and Akt activation after SDF-1 treatment ($P < 0.05$). In contrast, extracellular signal-regulated kinase, p38, signal transducer and activator of transcription 3, and Janus tyrosine kinase-1 NSC activation levels did not significantly change in response to SDF-1 treatment in either strain (not shown).

In addition to these differences, C57 NSCs were found to exhibit no appreciable increase in their migratory response to rSDF-1 compared with the robust increase in migration rate in response to rSDF-1 observed in CD-1 NSCs. In addition, in coculture with brain-derived microvascular endothelial cells and in culture of SVZ tissue sections, C57 NSCs do not exhibit any inhibition of their

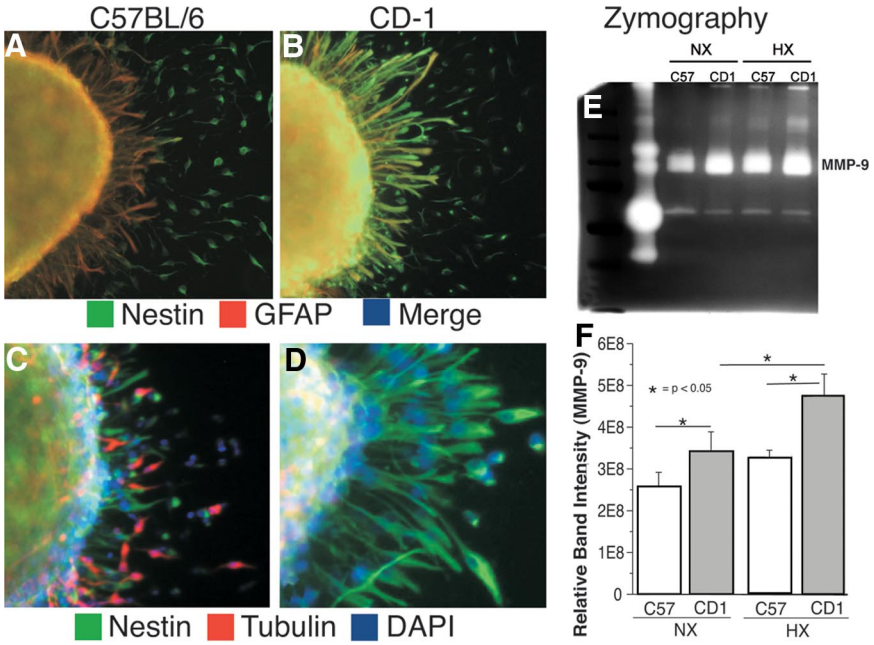

Figure 5. **A** and **B:** Confocal images of immunofluorescence staining of C57 (**A**) and CD-1 (**B**) neurospheres with nestin (green) and GFAP (red) after 48 hours of hypoxia. **C** and **D:** Confocal images of immunofluorescence staining of C57 (**C**) and CD-1 (**D**) neurospheres with nestin (green), β-tubulin III (red), and 4,6-diamidino-2-phenylindole (DAPI) (blue) after 48 hours of hypoxia. **E:** Representative zymography experiment of C57 and CD-1 NSCs cultured in normoxic (Nx) and hypoxic (Hx) conditions illustrating MMP-9 levels. **F:** Quantization of three zymography experiments illustrating increased activity of MMP-9 in the CD-1 NSCs.

migratory rate in response to addition of anti-SDF-1. In contrast, CD-1 NSCs exhibit significant blunting of their migratory rate in response to addition of anti-SDF-1 (Figure 4, E–H). These data are consistent with a differential responsiveness to SDF-1 engagement of CXCR4 in the NSCs of these two mouse strains that affects their migration rates and possibly their abilities to recover from hypoxic insult.

CD-1 and C57 NSCs Exhibit Distinct Neuronal Differentiation and MMP Expression Patterns

After a stimulus to migrate, CD-1 and C57 NSCs migrating outward from neurospheres exhibit unique differentiation and MMP profiles. Specifically, whereas migrating CD-1 NSCs retain their robust nestin staining and exhibit only minimal GFAP staining and no appreciable β-tubulin III staining (Figure 5, B and D), migrating C57 NSCs exhibit decreased nestin staining and increased GFAP and β-tubulin III staining (Figure 5, A and C). Interestingly, CD-1 NSCs exhibit increased MMP-9 activity in response to hypoxic conditions, whereas C57 NSCs exhibit only a nonstatistically significant change (Figure 5, E and F). These data are consistent with an earlier glial and neuronal differentiation, possibly resulting in decreased migration and recovery from reduction in O_2% (hypoxic insult) in C57 mice.

Adult CD-1 and C57 Mice Exhibit Significant Differences in Their Behavior after 8 Days of Hypoxic Insult (10% O_2) at P3 to P11

Although the previous differences between C57 and CD-1 pups and NSCs support our hypothesis,[14,31] the differences measured were all obtained over a relatively short time period of P0 through P11. As the variable recovery from chronic hypoxic insult in the premature infant population is known to occur over several years, we are now testing the animals over a longer time period (P40 through P120) to better mimic the human condition. Recently, we assessed the SVZ vascular densities of C57 and CD-1 mice reared in normoxic conditions from P0 to P40 and mice reared in hypoxic conditions (O_2 = 10%) from P3 to P11, followed by normoxic conditions until P40.

After the hypoxic insult, both strains exhibit a decrease in SVZ vascular density at P11 (Figure 6A).[37] This decrease in vessel density is thought to be due to the increased apoptosis noted in the SVZ microvasculature after the hypoxic period (Table 1).[14] However, at P17 significantly more angiogenesis was noted (illustrated by increased $\alpha v\beta 3$ staining of angiogenic sprouts) in the CD-1 pups (data not shown). At P40, although both strains exhibit increased vascular density compared with that at P11, the CD-1 mice exhibit significantly greater SVZ vascular density than the C57 cohort. In contrast, SVZ NSC proliferation (assessed by 5-bromo-2′-deoxyuridine incorporation), although decreased in both strains at P11 after hypoxia, was noted to be decreased at P40 compared with P11 under normoxic conditions. This decrease is consistent with the normally occurring pruning of neurons in the postnatal period of brain development and maturation observed in rodents.[38] However, at P40 in both normoxic- and hypoxic-reared animals, the CD-1 mice exhibited greater NSC proliferation (Figure 6B).[37] These findings i) are consistent with persistent differences in the recovery phase in these two mouse strains[39] and ii) confirm the concept of neurovascular coupling (a dynamic coordinated interaction of neurogenesis and angiogenesis observed in normal brain and in a wide variety of disease states including hypertension, stroke, and Alzheimer's disease.[40–43]

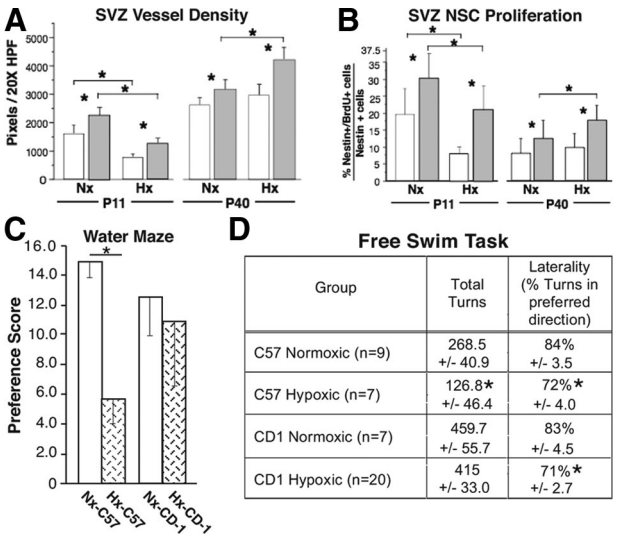

Group	Total Turns	Laterality (% Turns in preferred direction)
C57 Normoxic (n=9)	268.5 +/- 40.9	84% +/- 3.5
C57 Hypoxic (n=7)	126.8* +/- 46.4	72%* +/- 4.0
CD1 Normoxic (n=7)	459.7 +/- 55.7	83% +/- 4.5
CD1 Hypoxic (n=20)	415 +/- 33.0	71%* +/- 2.7

Figure 6. A–D: Adult CD-1 and C57 mice exhibit significant differences in their SVZ vascular density, NSC proliferation and behavior after 8 days of hypoxic insult (10% O_2) at P3 to P11. **A:** Quantitation of platelet endothelial cell adhesion molecule 1 (PECAM-1) immunohistochemical staining of normoxic (Nx) and hypoxic (Hx) P11 and P40 C57 and CD-1 SVZs of relative vessel densities (PECAM-1-positive structures) in the two mouse strains (open boxes, C57; shaded boxes, CD-1), illustrating the more robust response of the CD-1 mice. $n = 6$; $^*P < 0.05$. **B:** Quantitation of 5-bromo-2′-deoxyuridine (BrdU)/nestin immunohistochemical staining of normoxic and hypoxic P11 and P40 C57 and CD-1 SVZs (open boxes, C57; shaded boxes, CD-1) illustrating a more robust response in the CD-1 mice. $n = 6$; $^*P < 0.05$. **C:** To assess the strength of learning after 8 days of training in the Morris water maze, a 60-second probe trial was given on the 9th day during which the hidden platform was removed. The total time spent in the platform (training) quadrant, as well as the other three quadrants was calculated from the video records and the PPS was determined. Probe preference reflects the time spent in the training quadrant (T) relative to time in the other three quadrants (opposite, right, and left) on the probe trial and is equal to $[(T - O) + (T - R) + (T - L)]/3$. Individual *t*-tests were run to compare the PPS between CD-1 hypoxic ($n = 11$) and normoxic mice ($n = 9$) and C57 normoxic ($n = 10$) and hypoxic mice ($n = 12$). C57 hypoxic mice had a significantly lower PPS score than C57 normoxic mice, whereas there was no significant difference between these groups for CD-1 mice. These data are consistent with a more profound effect of early hypoxia on spatial memory in C57 than in CD-1 mice. $^*P < 0.001$. **D:** Mice were assessed using the free swim test at approximately 4 months of age. Over three 5-minute test sessions spaced 48 hours apart, the swimming activity of each mouse was videotaped, and the direction of swimming (clockwise or counterclockwise) and extent of swimming in each direction was scored in 30-degree increments. Each movement of 30 degrees in one direction was scored as a turn. The degree of laterality was calculated as the percentage of turns in the preferred direction of swimming. Both C57 and CD-1 hypoxic mice had significantly lower lateralization scores compared with normoxic mice. In addition, hypoxic C57 but not CD-1 mice made fewer turns, suggesting an additional effect on the emotional responses of these animals not present for CD-1 mice. $^*P < 0.05$. Data for C57 mice have been published previously in Chahboune et al.[37]

Further complementing our *in vivo* and *in vitro* biochemical analyses, we have begun behavioral studies with the aim of correlating changes in biochemical parameters with changes in behavior. The extent to which modifications in cortical and hippocampal organization occur as a result of hypoxia are also reflected in alterations of complex behaviors such as learning and memory, which were examined with the Morris water maze hidden platform task. The percentage of time mice spent swimming in the platform quadrant during the probe trial (PPS) was used as a measure of strength of initial learning. *t*-tests comparing the probe preference scores revealed that normoxic C57 mice spent significantly more time in the training quadrant than hypoxic-reared mice ($P < 0.001$) (Figure 6C)[37], whereas no significant difference was found for the score of the CD-1 normoxic and hypoxic groups.

Consistent with our biochemical analyses, the results of the behavioral analysis looking at open-field activity and spatial memory using the Morris water maze suggest that there are substantial differences in the impact of 8 days of hypoxia on the behavior of CD-1 versus C57 mice, with CD-1 mice being less adversely affected. However, analysis of these groups using the free swim task suggests that the CD-1 mice are not immune to the impact of hypoxia on certain classes of behavioral capacity and performance. Studies using the free-swimming test indicate that variations in rotational preference and lateralization for this task are linked to patterns of callosal connectivity and behavioral lateralization of the cerebral hemispheres. For example, mice with callosal agenesis[18,44] or transection of the corpus callosum[19] exhibit greater laterality in this task than normal mice. Further, the earlier the age at which callosal alteration occurs, the greater the impact on long-term laterality.[19] Our analysis revealed that CD-1 and C57 hypoxic mice were significantly less lateralized in their swimming preferences than normoxic mice. In addition, the total number of turns for hypoxic C57 mice was significantly reduced compared with that for normoxic controls (Figure 6D).[37] The effect of hypoxia on total turns in the C57 animals may reflect an additional effect on the emotional responses of these animals not apparent in the CD-1 mice, which is consistent with the reduced time exploring the center of the area in our open-field testing of these mice.

These findings not only i) are consistent with persistent differences in the SVZ NSC and vascular recovery phase in these two mouse strains and ii) confirm the concept of

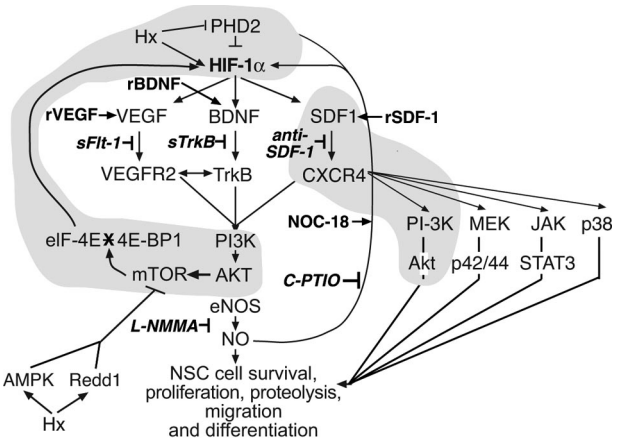

Figure 7. Current working model of the signaling pathway components (shaded areas) that are differentially regulated in C57 and CD-1 pup brain tissues and cultured NSCs under normoxic and hypoxic (Hx) conditions. Inducers rBDNF, rVEGF, rSDF-1 are shown in bold type; inhibitors sFLT-1, sTrkB, anti-SDF-1, C-PTIO, L-N^G-monomethyl arginine citrate (L-NMMA) are shown in bold italic type. NO, nitric oxide; eNOS, endothelial nitric oxide synthase; MEK, mitogen-activated protein kinase kinase; Janus tyrosine kinase (JAK), STAT, signal transducer and activator of transcription; AMPK, AMP-activated protein kinase. (Drawn from data and concepts presented in Nakamura et al,[49] Liu and Simon,[51] van den Beucken et al,[52] Simon et al,[53] Li et al,[14, 25] and this study). sFLT-1, soluble fms-like tyrosine kinase-1; sTrkB, soluble neurotrophic tyrosine kines, receptor, type 2; c-PTIO, carboxy-2-phenyl-4, 4, 5, 5 tetramethylimidazoline-1-oxyl-3 oxide.

neurovascular coupling in the SVZ but they also suggest iii) a correlation of behaviors with the responsiveness/recovery of the SVZ in these two mouse strains.

Discussion

Our studies revealed that CD-1 NSC self-renewal ability is appreciably greater than that observed in C57 NSCs and that this may, in part, explain the differences in behavior observed in these two strains after exposure to hypoxia. In addition to our previous findings, which documented significant differences in HIF-1α, BDNF, VEGF, SDF-1, neuropilin-1, and CXCR4 expression in brain tissues and NSC lysates in these two strains,[14] our current studies showed that CD-1 NSCs, in addition to exhibiting less apoptosis after hypoxic insult, exhibit increased HIF-1α mRNA and protein as well as increased HIF-1α and decreased PHD2 protein levels in their nuclear fractions compared with those in C57 cells, which is consistent with increased transcription and translation and decreased degradation of HIF-1α in the CD-1 NSCs.

The increased translation of HIF-1α was found to be mTOR-dependent. The role of mTOR in the modulation of cellular responses to hypoxic insult is complex and probably cell type- and culture condition-dependent,[45] with evidence consistent with either HIF-1α translation being mTOR-independent[46] or mTOR-dependent, with mTOR either being inhibited by hypoxic insult via AMP-activated protein kinase and Redd1 pathways[47,48] or being activated via growth factor pathways.[45,49,50] Our data are consistent with a growth factor (BDNF, VEGF, and SDF-1)-mediated stimulation of mTOR via the PI3K/Akt pathway[14,25] (illustrated in Figure 7).[49,51–53]

In this study, we found that C57 and CD-1 NSCs exhibit similar proliferative and survival responses but differential migratory responses[32,54,55] to exogenous rSDF-1. When examined, selected known signaling components downstream of CXCR4,[34] including PI3K and Akt, but not extracellular signal-regulated kinase, Janus tyrosine kinase-1, signal transducer and activator of transcription-1, and p38, were found to be differentially phosphorylated in response to exogenous rSDF-1 in the two mouse strains. Specifically, C57 NSCs did not exhibit any significant induction after treatment with rSDF-1, whereas CD-1 NSCs exhibited significant PI3K and Akt activation.

C57 NSCs were also found to exhibit a blunted migratory responsiveness to SDF-1 (known to mediate neural progenitor cell motility after ischemia[56]) and decreased induction of MMP-9 (known to be involved in modulating neuroblast migration from the SVZ after stroke and ischemia[57,58]) compared with CD-1 NSCs. This finding is consistent with our hypothesis that the behavioral data exhibited by the C57 pups may be a consequence of their relative lower proliferative and migratory rates and higher susceptibility to undergo apoptosis in response to a reduction in O_2% because of their relatively blunted HIF-1α response compared with that of CD-1 pups and in part mediated by their blunted response to SDF-1.[59]

Interestingly, we observed increased glial and neuronal differentiation (a process known to be affected by SDF-1-CXCR4 signaling)[60] in C57 NSCs after radial migration outward from cultured neurospheres, suggesting that in addition to the other above-mentioned factors that may influence their responsiveness to a hypoxic insult, the earlier progression of the c57 NSCs to neuronal differentiation (evidenced by increased GFAP and β-tubulin III expression) may influence their migration and hence their ability to affect optimal recovery after a hypoxic insult *in vivo*.

Although contributing to variability in responsiveness to hypoxic insult in these mouse strains, the signaling pathways discussed here probably account for only a subset of potential differences between these two strains (and probably the variable recovery from hypoxic insult observed in the very low birth weight infant human population). Other potential mechanisms involved in eliciting a differential response/recovery from hypoxic insult may include differences in VEGF expression and induction,[61] differences in BDNF expression level, induction,[62] and polymorphism[63] and polymorphisms in several cytokines and extracellular matrix components.[64,65]

Thus, in this report we have documented significant differences in HIF-1α translation and responsiveness to SDF-1 in C57 and CD-1 NSCs (shaded aspects of the signaling pathways are illustrated in Figure 7).[48,50–52] Specifically, C57 NSCs exhibit blunted HIF-1α translation in response to a reduced O_2 culture environment. Similarly, C57 NSCs also display an earlier neuronal differentiation and a diminished migratory response to exogenous rSDF-1. In addition, the strain differences in SVZ vessel density and NSC proliferation observed immediately after the P3 to P11 hypoxic insult are manifested in the adult animals at P40. These strain differences may provide insights needed to develop a better understanding of NSC behavior during the variable repair/recovery observed after chronic hypoxic injury in the very low birth weight newborn population, as well as in adult populations after stroke and during neurodegeneration. Investigations using these mouse strains and cells derived from them may also aid in the development of rational therapeutic modalities that may affect recovery beneficially in these at-risk populations.

Acknowledgments

We thank Mr. Jake Kravitz for his excellent technical assistance and the members of the Madri Laboratory for their help.

References

1. Wilson-Costello D, Friedman H, Minich N, Fanaroff AA, Hack M: Improved survival rates with increased neurodevelopmental disability for extremely low birth weight infants in the 1990s. Pediatrics 2005, 115:997–1003
2. Tyson JE, Saigal S: Outcomes for extremely low-birth-weight infants: disappointing news. JAMA 2005, 294:371–373
3. Saigal S, Stoskopf B, Streiner D, Boyle M, Pinelli J, Paneth N, Goddeeris J: Transition of extremely low-birth-weight infants from adolescence to young adulthood: comparison with normal birth-weight controls. JAMA 2006, 295:667–675

4. Hack M, Flannery DJ, Schluchter M, Cartar L, Borawski E, Klein N: Outcomes in young adulthood for very-low-birth-weight infants. N Engl J Med 2002, 346:149–157
5. Saigal S, Doyle LW: An overview of mortality and sequelae of preterm birth from infancy to adulthood. Lancet 2008, 371:261–269
6. Schafer RJ, Lacadie C, Vohr B, Kesler SR, Katz KH, Schneider KC, Pugh KR, Makuch RW, Reiss AL, Constable RT, Ment LR: Alterations in functional connectivity for language in prematurely born adolescents, Brain 2009, 132:661–670
7. Ment LR, Constable RT: Injury and recovery in the developing brain: evidence from functional MRI studies of prematurely-born children, Nat Clin Prac Neurol 2007, 3:558–571
8. Bassan H, Feldman HA, Limperopoulos C, Benson CB, Ringer SA, Veracruz E, Soul JS, Volpe JJ, du Plessis AJ: Periventricular hemorrhagic infarction: risk factors and neonatal outcome. Pediatr Neurol 2006, 35:85–92
9. Paul DA, Leef KH, Locke RG, Bartoshesky L, Walrath J, Stefano JL: Increasing illness severity in very low birth weight infants over a 9-year period. BMC Pediatr 2006, 6:2
10. Cooke RW: Preterm mortality and morbidity over 25 years. Arch Dis Child Fetal Neonatal Ed 2006, 91:F293–F294
11. Curristin SM, Cao A, Stewart WB, Zhang H, Madri JA, Morrow JS, Ment LR: Disrupted synaptic development in the hypoxic newborn brain, Proc Natl Acad Sci USA 2002, 99:15729–15734
12. Fagel DM, Ganat Y, Silbereis J, Ebbitt T, Stewart W, Zhang H, Ment LR, Vaccarino FM: Cortical neurogenesis enhanced by chronic perinatal hypoxia. Exp Neurol 2006, 199:77–91
13. Warner-Schmidt JL, Duman RS: Hippocampal neurogenesis: opposing effects of stress and antidepressant treatment. Hippocampus 2006, 16:239–249
14. Li Q, Michaud M, Stewart W, Schwartz M, Madri JA: Modeling the neurovascular niche: murine strain differences mimic the range of responses to chronic hypoxia in the premature newborn. J Neurosci Res 2008, 86:1227–1242
15. Barrett RD, Bennet L, Davidson J, Dean JM, George S, Emerald BS, Gunn AJ: Destruction and reconstruction: hypoxia and the developing brain. Birth Defects Res C Embryo Today 2007, 81:163–176
16. Brazel CY, Rosti RT, Boyce S, Rothstein RP, Levison SW: Perinatal hypoxia/ischemia damages and depletes progenitors from the mouse subventricular zone. Dev Neurosci 2004, 26:266–274
17. Jonasson Z: Meta-analysis of sex differences in rodent models of learning and memory: a review of behavioral and biological data. Neurosci Biobehav Rev 2005, 28:811–825
18. Filgueiras CC, Manhães AC: Effects of callosal agenesis on rotational side preference of BALB/cCF mice in the free swimming test. Behav Brain Res 2004, 155:13–25
19. Manhães AC, Abreu-Villaca Y, Schmidt SL, Filgueiras CC: Neonatal transection of the corpus callosum affects rotational side preference in adult Swiss mice. Neurosci Lett 2007, 415:159–163
20. Schalomon PM, Wahlsten D: Wheel running behavior is impaired by both surgical section and genetic absence of the mouse corpus callosum. Brain Res Bull 2002, 57:27–33
21. Morris RGM, Garrud P, Rawlins JNP, O'Keef J: Place navigation impaired in rats with hippocampal lesions. Nature 1982, 297:681–683
22. Khanna S, Roy S, Maurer M, Ratan R, Sen CK: Oxygen-sensitive reset of hypoxia-inducible factor transactivation response: prolyl hydroxylases tune the biological normoxic set point. Free Radic Biol Med 2006, 40:2147–2154
23. Graesser D, Solowiej A, Bruckner M, Osterweil E, Juedes A, Davis S, Ruddle NH, Engelhardt B, Madri JA: Altered vascular permeability and early onset of experimental autoimmune encephalomyelitis in PECAM-1-deficient mice. J Clin Invest 2002, 109:383–392
24. Ford MC, Bertram JP, Hynes SR, Michaud M, Li Q, Young M, Segal SS, Madri JA, Lavik EB: A macroporous hydrogel for the coculture of neural progenitor and endothelial cells to form functional vascular networks in vivo, Proc Natl Acad Sci USA 2006, 103:2512–2517
25. Li Q, Ford MC, Lavik EB, Madri JA: Modeling the neurovascular niche: vEGF- and BDNF-mediated cross-talk between neural stem cells and endothelial cells: an in vitro study. J Neurosci Res 2006, 84:1656–1668
26. Durbec P, Franceschini I, Lazarini F, Dubois-Dalcq M: In Vitro Migration Assays of Neural Stem Cells. Edited by Weiner LP. Totowa, NJ, Humana Press, 2008, pp 213–225
27. Haas TL, Madri JA: Extracellular matrix-driven matrix metalloproteinase production in endothelial cells: implications for angiogenesis. Trends Cardiovasc Med 1999, 9:70–77
28. Haas TL, Milkiewicz M, Davis SJ, Zhou AL, Egginton S, Brown MD, Madri JA, Hudlicka O: Matrix metalloproteinase activity is required for activity-induced angiogenesis in rat skeletal muscle. Am J Physiol Heart Circ Physiol 2000, 279:H1540–H1547
29. Esparza J, Kruse M, Lee J, Michaud M, Madri JA: MMP-2 null mice exhibit an early onset and severe experimental autoimmune encephalomyelitis due to an increase in MMP-9 expression and activity. FASEB J 2004, 18:1682–1691
30. Sheldon RA, Sedik C, Ferriero DM: Strain-related brain injury in neonatal mice subjected to hypoxia-ischemia. Brain Res 1998, 810:114–122
31. Ward NL, Moore E, Noon K, Spassil N, Keenan E, Ivanco TL: LaManna JC: Cerebral angiogenic factors, angiogenesis, and physiological response to chronic hypoxia differ among four commonly used mouse strains. J Appl Physiol 2007, 102:1927–1935
32. Stumm R, Höllt V: CXC chemokine receptor 4 regulates neuronal migration and axonal pathfinding in the developing nervous system: implications for neuronal regeneration in the adult brain. J Mol Endocrinol 2007, 38:377–382
33. Claps CM, Corcoran KE, Cho KJ, Rameshwar P: Stromal derived growth factor-1α as a beacon for stem cell homing in development and injury. Curr Neurovasc Res 2005, 2:319–329
34. Kucia M, Jankowski K, Reca R, Wysoczynski M, Bandura L, Allendorf DJ, Zhang J, Ratajczak J, Ratajczak MZ: CXCR4-SDF-1 signalling, locomotion, chemotaxis and adhesion. J Mol Histol 2004, 35:233–245
35. Guan K-L, Rao Y: Signalling mechanisms mediating neuronal responses to guidance cues. Nat Rev Neurosci 2003, 4:941–956
36. Busillo JM, Benovic JL: Regulation of CXCR4 signaling. Biochim Biophys Acta 2007, 1768:952–963
37. Chahboune H, Ment LR, Stewart WB, Rothman DL, Vaccarino FM, Hyder F, Schwartz ML: Hypoxic injury during neonatal development in murine brain: correlation between in vivo DTI findings and behavioral assessment. Cereb Cortex 2009, DOI: 10.1093/cercor/bhp068
38. Ogunshola OO, Stewart WB, Mihalcik V, Solli T, Madri JA, Ment LR: Neuronal VEGF expression correlates with angiogenesis in postnatal developing rat brain. Brain Res Dev Brain Res 2000, 119:139–153
39. Als H, Duffy FH, McAnulty GB, Rivkin MJ, Vajapeyam S, Mulkern RV, Warfield SK, Huppi PS, Butler SC, Conneman N, Fischer C, Eichenwald EC: Early experience alters brain function and structure. Pediatrics 2004, 114:1738–1739
40. Louissaint A, Rao S, Leventhal C, Goldman SA: Coordinated interaction of neurogenesis and angiogenesis in the adult songbird brain. Neuron 2002, 34:945–960
41. Ohab JJ, Fleming S, Blesch A, Carmichael ST: A neurovascular niche for neurogenesis after stroke. J Neurosci 2006, 26:13007–13016
42. Pereira AC, Huddleston DE, Brickman AM, Sosunov AA, Hen R, McKhann GM, Sloan R, Gage FH, Brown TR, Small SA: An in vivo correlate of exercise-induced neurogenesis in the adult dentate gyrus, Proc Natl Acad Sci USA 2007, 104:5638–5644
43. Girouard H, Iadecola C: Neurovascular coupling in the normal brain and in hypertension, stroke, and Alzheimer disease. J Appl Physiol 2006, 100:328–335
44. Filgueiras CC, Manhães AC: Increased lateralization in rotational side preference in male mice rendered acallosal by prenatal gamma irradiation. Behav Brain Res 2005, 162:289–298
45. Takei N, Inamura N, Kawamura M, Namba H, Hara K, Yonezawa K, Nawa H: Brain-derived neurotrophic factor induces mammalian target of rapamycin-dependent local activation of translation machinery and protein synthesis in neuronal dendrites. J Neurosci 2004, 24:9760–9769
46. Pore N, Jiang Z, Shu HK, Bernhard E, Kao GD, Maity A: Akt1 activation can augment hypoxia-inducible factor-1alpha expression by increasing protein translation through a mammalian target of rapamycin-independent pathway. Mol Cancer Res 2006, 4:1–9
47. Brugarolas J, Lei K, Hurley RL, Manning BD, Reiling JH, Hafen E, Witters LA, Ellisen LW, Kaelin WG Jr: Regulation of mTOR function in response to hypoxia by REDD1 and the TSC1/TSC2 tumor suppressor complex. Genes Dev 2004, 18:2893–2904
48. Shaw RJ, Bardeesy N, Manning BD, Lopez L, Kosmatka M, DePinho RA, Cantley LC: The LKB1 tumor suppressor negatively regulates mTOR signaling. Cancer Cell 2004, 6:91–99
49. Nakamura K, Martin KC, Jackson JK, Beppu K, Woo CW, Thiele CJ: Brain-derived neurotrophic factor activation of TrkB induces vascular

endothelial growth factor expression via hypoxia-inducible factor-1α in neuroblastoma cells. Cancer Res 2006, 66:4249–4255
50. Liao L, Pilotte J, Xu T, Wong CC, Edelman GM, Vanderklish P, Yates JR 3rd: BDNF induces widespread changes in synaptic protein content and up-regulates components of the translation machinery: an analysis using high-throughput proteomics. J Proteome Res 2007, 6:1059–1071
51. Liu L, Simon MC: Regulation of transcription and translation by hypoxia. Cancer Biol Ther 2004, 3:492–497
52. van den Beucken T, Koritzinsky M, Wouters BG: Translational control of gene expression during hypoxia. Cancer Biol Ther 2006, 5:749–755
53. Simon MC, Liu L, Barnhart BC, Young RM: Hypoxia-induced signaling in the cardiovascular system. Annu Rev Physiol 2008, 70:51–71
54. Stumm RK, Zhou C, Ara T, Lazarini F, Dubois-Dalcq M, Nagasawa T, Höllt V, Schulz S: CXCR4 regulates interneuron migration in the developing neocortex. J Neurosci 2003, 23:5123–5133
55. Tan W, Palmby TR, Gavard J, Amornphimoltham P, Zheng Y, Gutkind JS: An essential role for Rac1 in endothelial cell function and vascular development. FASEB J 2008, 22:1829–1838
56. Robin AM, Zhang ZG, Wang L, Zhang RL, Katakowski M, Zhang L, Wang Y, Zhang C, Chopp M: Stromal cell-derived factor 1α mediates neural progenitor cell motility after focal cerebral ischemia. J Cereb Blood Flow Metab 2006, 26:125–134
57. Lee S-R, Kim HY, Rogowska J, Zhao BQ, Bhide P, Parent JM, Lo EH: Involvement of matrix metalloproteinase in neuroblast cell migration from the subventricular zone after stroke. J Neurosci Res 2006, 26:3491–3495
58. Kang SS, Kook JH, Hwang S, Park SH, Nam SC, Kim JK: Inhibition of matrix metalloproteinase-9 attenuated neural progenitor cell migration after photothrombotic ischemia. Brain Res 2008, 1228:20–26
59. Tang CH, Tan TW, Fu WM, Yang RS: Involvement of matrix metalloproteinase-9 in stromal cell-derived factor-1/CXCR4 pathway of lung cancer metastasis. Carcinogenesis 2008, 29:35–43
60. Peng H, Kolb R, Kennedy JE, Zheng J: Differential expression of CXCL12 and CXCR4 during human fetal neural progenitor cell differentiation. J Neuroimmune Pharmacol 2007, 2:251–258
61. Chalothorn D, Clayton JA, Zhang H, Pomp D, Faber JE: Collateral density, remodeling, and VEGF-A expression differ widely between mouse strains. Physiol Genomics 2007, 30:179–191
62. Chouthai NS, Sampers J, Desai N, Smith GM: Changes in neurotrophin levels in umbilical cord blood from infants with different gestational ages and clinical conditions. Pediatr Res 2003, 53:965–969
63. Egan MF, Kojima M, Callicott JH, Goldberg TE, Kolachana BS, Bertolino A, Zaitsev E, Gold B, Goldman D, Dean M, Lu B, Weinberger DR: The BDNF val66met polymorphism affects activity-dependent secretion of BDNF and human memory and hippocampal function. Cell 2003, 112:257–269
64. Baier RJ: Genetics of perinatal brain injury in the preterm infant. Front Biosci 2006, 11:1371–1387
65. Back SA: Perinatal white matter injury: the changing spectrum of pathology and emerging insights into pathogenetic mechanisms. Ment Retard Dev Disabil Res Rev 2006, 12:129–140